Search method for coincident events from LIGO and IceCube detectors

Yoichi Aso[1]**, Zsuzsa Márka**[1]**, Chad Finley**[2]**, John Dwyer**[1]**, Kei Kotake**[3]**, Szabolcs Márka**[1]

[1]Department of Physics, Columbia University, New York, NY, 10027, USA
[2]Department of Physics, University of Wisconsin, Madison,WI, 53706, USA
[3]Division of Theoretical Astronomy, National Astronomical Observatory of Japan, Mitaka, Tokyo, Japan

E-mail: `aso@astro.columbia.edu`

Abstract. We present a coincidence search method for astronomical events using gravitational wave detectors in conjunction with other astronomical observations. We illustrate our method for the specific case of LIGO gravitational wave detector and the IceCube neutrino detector. Event triggers which appear in both detectors within a certain time window are selected as time coincident events. Then the spatial overlap of reconstructed event directions is evaluated by an unbinned maximum likelihood method. Our method was tested by Monte Carlo simulations using simulated LIGO and IceCube events. We estimated a typical false alarm rate of the analysis to be 1 event per 435 years. This would allow us to relax the event trigger thresholds of the individual detectors and improve the detection capability.

Submitted to: *Class. Quantum Grav.*

1. Introduction

There are several interferometric gravitational wave (GW)[1] detectors around the world, such as LIGO[2], TAMA[3], GEO[4] and VIRGO[5], currently in operation. Those detectors monitor the relative displacement of mirrors (test masses) in response to distortions induced by gravitational waves. Since the interaction of gravitational waves with matter is extremely weak, expected signals even from very strong gravitational wave sources are very small. In order to declare a detection, we have to find a small signal in overwhelming background noise with high confidence. Generally, the output from the detector contains glitches which are not associated with gravitational waves but rather caused by various local disturbances such as laser noises, seismic excitations, etc. In order to search for GW bursts, which are gravitational waves of short duration, it is therefore important to distinguish gravitational wave signals from noise glitches without prior knowledge of signal waveforms.

One way to pick up gravitational wave signals of unknown waveform from the noise background is to find coincidences between independent detectors. We can

reject a large portion of background events by comparing the arrival time and other properties (frequency, duration, etc) of the signals detected by independent gravitational wave detectors [6, 7, 8]. Additionally, event lists from other astronomical observations, such as Gamma-Ray Bursts (GRB), optical supernovae, neutrinos, etc., can be used to find events that may be associated with GW bursts with an increased likelihood [9, 10, 11, 12, 13]. Moreover, strict coincidence requirements allow us to investigate candidate events at lower Signal-to-Noise Ratios (SNRs) while maintaining a low False Alarm Rate (FAR). Here, we propose a method for coincidence analysis of gravitational wave data with other detectors and illustrate it for the case of LIGO gravitational wave detector and the IceCube neutrino detector.

LIGO is a network of interferometric gravitational wave detectors consisting of three interferometers‡ in the USA [14]. Two interferometers (4 km and 2 km long ones) are co-located in Hanford, WA and another 4 km interferometer is located in Livingston, LA. They have now achieved the design sensitivity [15].

IceCube [16] is a cubic kilometer-scale neutrino detector under construction at the geographic South Pole. Its primary mission is the search for high energy extraterrestrial neutrinos. When completed, the detector will consist of an array of 4800 digital optical modules, attached to 80 strings submerged within the Antarctic ice. Currently the detector is taking data with more than 90 % livetime, except during a few months each year for construction and commissioning of new strings. IceCube is optimized to look "down," using the Earth as a screen to block all particles except neutrinos; thus its field of view is the northern hemisphere. Neutrino arrival directions are resolved with a median error between $1°$ and $2°$ [17].

In this analysis, we look for astrophysical sources which produce both gravitational wave and high energy neutrino bursts. One example of the possible sources is a gamma-ray burst (GRB). Thanks to the *Swift* satellite [18], there is accumulating observational evidence suggesting the association of long GRBs with the death of massive stars and supernova-like events (e.g. SN2006aj and GRB060218 [19], see also [20]). The collapsar model [21] is widely accepted for explaining long GRBs and stellar collapse. During the gravitational collapse of rapidly rotating stars, gravitational waves are emitted (see [22] for a review). Fireballs heated by neutrinos from the accretion disk are considered to produce the prompt gamma-ray emissions at first [23]. Subsequently in the prompt and afterglow phases, high energy neutrinos are expected to be produced by accelerated protons in relativistic shocks (see [24, 25] for reviews). High energy neutrinos could be emitted also from short-duration GRBs, which are thought to be the outcome of neutron star mergers [26]. There is currently limited knowledge both observationally and theoretically about the details of the astrophysical process from the gravitational collapse/merger of compact objects through the black hole formation to the formation of fireballs. Coincident observations of gravitational waves and neutrinos from those events could therefore make an important contribution to the understanding of such phenomena.

Apart from GRBs, there may be other (unknown) classes of sources which produce bright bursts both in gravitational waves and neutrinos. Since our proposed method is not specific to any source type, our search will be able to set an upper limit for the population of any sources that produce nearly simultaneous bursts of gravitational waves and high energy neutrinos within the detection range of LIGO and IceCube.

---

‡ From now on, we treat the network of the three LIGO interferometers as one detector and use the word "detector" to refer to them as a whole. To refer to individual LIGO interferometers, we always use the word "interferometer" to avoid confusion.
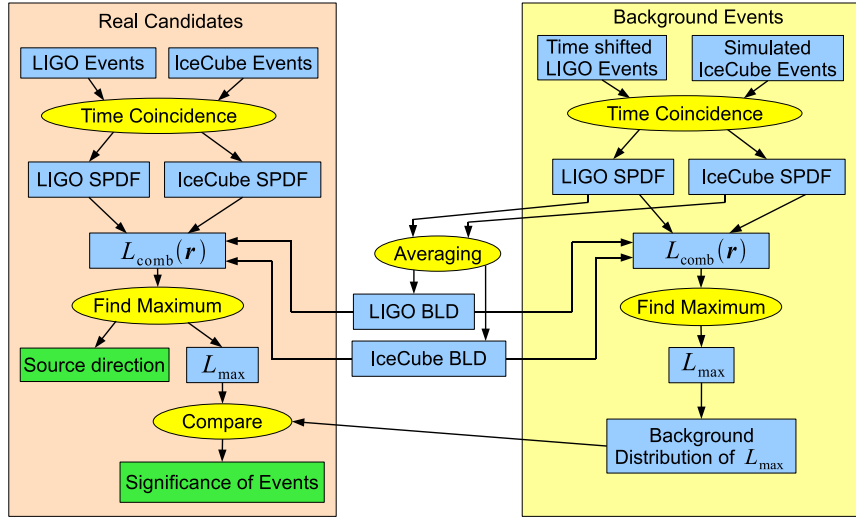
Figure 1. Outline of the analysis pipeline. SPDF: Spatial Probability Distribution Function. BLD: Background Likelihood Distribution. $L_{\mathrm{comb}}(\boldsymbol{r})$: Combined Likelihood Distribution. L_{max}: The maximum value of L_{comb}.

We may also discover a previously unknown astrophysical phenomenon, when such events are found at a high confidence level.

In our search method, the data streams from the LIGO interferometers are processed by a trigger generation pipeline, which generates a list of possible gravitational wave triggers for each interferometer. Then we compare the trigger lists from LIGO interferometers to generate a coincident LIGO event list, which contains the arrival time and the source direction of each candidate event. The LIGO event list is compared with an event list from the IceCube detector which also contains the timing and source direction information of the events. From the event lists we choose pairs of LIGO-IceCube events which lie within a certain time interval as time coincident events. Then the spatial overlap between the LIGO and IceCube events is statistically evaluated to obtain the significance of the coincident event.

Because of the very different nature and geographical location of the two detectors, it is extremely unlikely that they share a same noise source. Therefore, the remaining possibility for time coincident trigger generation in both detectors, other than real astronomical events, is accidental coincidence. Furthermore, the chance for two time-coincident noise triggers to generate overlapping reconstructed directions on the sky is also exceedingly small. By the combination of the timing and directional coincidence discrimination, we can expect that most background events will be rejected and the FAR will be significantly reduced.

2. Coincidence analysis

The outline of the proposed analysis method is shown in figure 1. The inputs to the analysis pipeline are LIGO and IceCube event trigger lists and a large number

of simulated background events. The output of the pipeline are the most plausible source direction and the statistical significance of each candidate event against the background noise events.

2.1. Event lists

Data streams from LIGO interferometers are processed by a trigger generation pipeline (e.g. [27, 28]) to generate a list of event candidates for each LIGO interferometer. We then compare the arrival times of the events from the LIGO interferometers and select events which appear in all the detectors with less than 10 ms time difference. 10 ms corresponds to the gravitational wave's travel time between the two LIGO sites, i.e. the maximum time delay allowed for a gravitational wave signal. If the trigger generation pipeline provides more information on the candidate events, such as dominant frequency, duration, etc., we also compare those parameters and reject events with large discrepancies.

This intra-LIGO coincidence can be applied between all three LIGO interferometers or any combination of two interferometers. From now on in this paper, we focus on the two-interferometer case using the Hanford 4 km (H1) and the Livingston 4 km (L1) interferometers, because the third interferometer (Hanford 2 km) is two times less sensitive than the others.

For later statistical treatments, a large number of background events are created, also from the LIGO data, in almost the same way. The only difference is that we introduce an artificial time shift between the trigger times from different interferometers to ensure that the resultant background event list does not contain real gravitational wave events.

A list of IceCube events is generated by the event reconstruction algorithm of IceCube. The event information used for this analysis is the time, the arrival direction, and its associated angular uncertainty. The background events for IceCube are produced by Monte Carlo simulations which imitate the properties of IceCube events.

2.2. Time coincidence

Once event lists from LIGO and IceCube are prepared, they are compared for inter-detector time coincidence. We look for pairs of LIGO and IceCube events which appear within a certain time window and register them as time-coincident combined events for further analysis.

A smaller time window can reject background events more efficiently. However, the size of the time window must be sufficiently large to allow intrinsic time delay between the two emission processes at the source. Since we do not assume any specific source model in this analysis, we propose to use several time windows e.g. 0.1, 1, 10 sec and also 1 day in the case of long GRB search.

2.3. Spatial coincidence

The LIGO-IceCube combined events which survive the time-coincidence discrimination are further processed in order to examine spatial coincidence by an unbinned maximum likelihood method.
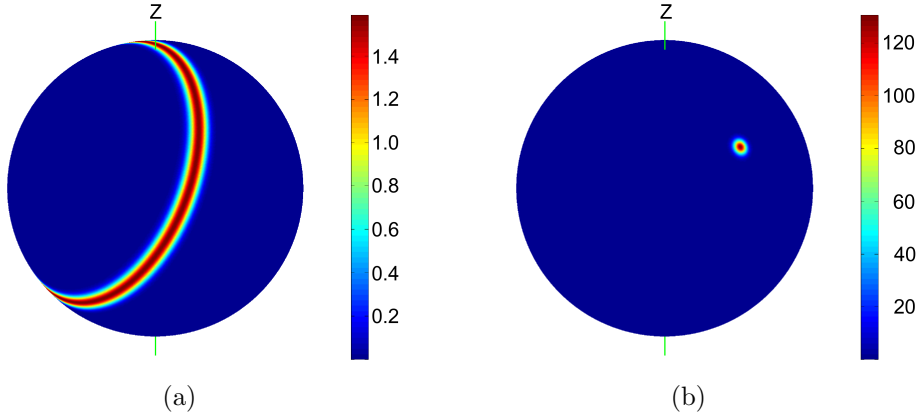
Figure 2. Examples of spatial probability distribution functions (SPDFs). (a) SPDF of a LIGO event with $\tau = 4\,\text{msec}$ and $\delta\tau = 440\,\mu\text{sec}$. (b) SPDF of an IceCube event with $\sigma_\nu = 2°$. The plots are shown in Earth based coordinates with the z-axis pointing along the north pole. Both SPDFs are normalized to 1 for integration over the sphere.

First, we calculate the Spatial Probability Distribution Function (SPDF) of each event from LIGO and IceCube. Taking a sky location $\boldsymbol{r}$ as an input, this function returns the probability of the actual source location being $\boldsymbol{r}$.

The source location of each LIGO event is reconstructed by measuring the arrival time difference τ of the signal between the two sites. Using the measured arrival time difference τ_{M}, we can constrain the possible source locations to a ring on the sky defined by a polar angle $\theta_{\text{ev}} = \cos^{-1}(c\tau_{\text{M}}/D)$ measured from the axis connecting the two LIGO sites (LIGO axis). Here, c is the speed of light and D is the distance between the two LIGO sites. Because the measured τ_{M} has uncertainty $\delta\tau$, the ring has a finite thickness. We assume that the probability distribution of the real time delay, τ, is a Gaussian around the measured time delay τ_{M} with the standard deviation $\delta\tau$. By changing the variate from τ to θ using $\theta = \cos^{-1}(c\tau/D)$, we get the SPDF for a LIGO event,

$$S_{\text{GW}}\left(\boldsymbol{r}; \theta_{\text{ev}}, \delta\tau\right) = A_{\text{GW}} \cdot \exp\left[-\frac{D^2\left(\cos\theta - \cos\theta_{\text{ev}}\right)^2}{2\delta\tau^2 c^2}\right], \tag{1}$$

$$\theta = \cos^{-1}\left(\frac{\boldsymbol{r} \cdot \boldsymbol{l}}{|\boldsymbol{r}| \cdot |\boldsymbol{l}|}\right), \tag{2}$$

where $\boldsymbol{l}$ is a vector parallel to the LIGO axis and θ is the angle between $\boldsymbol{r}$ and the LIGO axis. $S_{\text{GW}}\left(\boldsymbol{r}; \theta_{\text{ev}}, \delta\tau\right)$ is normalized to unity over the whole sky by a normalization factor A_{GW}. An example of a LIGO event is shown in figure 2 (a).

For the SPDF of an IceCube event we use a two-dimensional Gaussian distribution on a sphere:

$$S_\nu\left(\boldsymbol{r}; \boldsymbol{r}_{\text{ev}}, \sigma_\nu\right) = A_\nu \cdot \exp\left(\frac{-\psi^2}{2\sigma_\nu^2}\right), \tag{3}$$

$$\psi = \cos^{-1}\left(\frac{\boldsymbol{r} \cdot \boldsymbol{r}_{\text{ev}}}{|\boldsymbol{r}| \cdot |\boldsymbol{r}_{\text{ev}}|}\right), \tag{4}$$

where $\boldsymbol{r}_{\mathrm{ev}}$ is the vector representing the reconstructed event direction and ψ is the angle between $\boldsymbol{r}$ and $\boldsymbol{r}_{\mathrm{ev}}$. A_{ν} is the normalization factor and σ_{ν} is the uncertainty of the reconstructed event direction. An example of an IceCube event is shown in figure 2 (b).

The distribution of background noise events is not uniform over the sky. The background likelihood distribution (BLD) is a function of a reconstructed event direction which returns a value proportional to the likelihood of a background event coming from this direction. The reconstructed event direction is specified by a polar angle θ_{ev} measured from the LIGO axis for LIGO events and by a vector $\boldsymbol{r}_{\mathrm{ev}}$ for IceCube events. There are two BLDs, $B_{\mathrm{GW}}(\theta_{\mathrm{ev}})$ and $B_{\nu}(\boldsymbol{r}_{\mathrm{ev}})$ corresponding to LIGO and IceCube detectors respectively. BLDs are obtained from histograms of reconstructed event directions, θ_{ev} and $\boldsymbol{r}_{\mathrm{ev}}$, for a large number of background events. The histograms are converted to BLDs by normalizing them to 1 for integration over the whole sky.

Finally, we calculate the combined likelihood distribution of a combined LIGO-IceCube event with the following formula:

$$L_{\mathrm{comb}}\left(\boldsymbol{r}\right) = \frac{S_{\mathrm{GW}}\left(\boldsymbol{r};\theta_{\mathrm{ev}},\delta\tau\right) \cdot S_{\nu}\left(\boldsymbol{r};\boldsymbol{r}_{\mathrm{ev}},\sigma_{\nu}\right)}{B_{\mathrm{GW}}(\theta_{\mathrm{ev}}) \cdot B_{\nu}(\boldsymbol{r}_{\mathrm{ev}})}. \tag{5}$$

$L_{\mathrm{comb}}\left(\boldsymbol{r}\right)$ has a bright spot on the sky when the reconstructed directions of LIGO and IceCube events have good overlap. We search for every direction on the sky and find a direction $\boldsymbol{r}_{\mathrm{max}}$ which gives the maximum value $L_{\mathrm{max}} = L_{\mathrm{comb}}\left(\boldsymbol{r}_{\mathrm{max}}\right) = \mathrm{Max}\left[L_{\mathrm{comb}}\left(\boldsymbol{r}\right)\right]$. L_{max} is a good measure of spatial coincidence and $\boldsymbol{r}_{\mathrm{max}}$ is the most likely source direction.

In order to evaluate the statistical significance of a given L_{max}, we first calculate the background distribution $P_{L_{\mathrm{max}}}^{\mathrm{BG}}\left(L_{\mathrm{max}}\right)$ of L_{max} using a large number of background events. $P_{L_{\mathrm{max}}}^{\mathrm{BG}}\left(L_{\mathrm{max}}\right)$ gives the probability of a background event having a particular L_{max}. Then the statistical significance of a candidate combined-event with $L_{\mathrm{max}} = L_{\mathrm{ev}}$ is measured by a number called p-value defined as follows:

$$p = \int_{L_{\mathrm{ev}}}^{\infty} P_{L_{\mathrm{max}}}^{\mathrm{BG}}\left(L_{\mathrm{max}}\right) dL_{\mathrm{max}}. \tag{6}$$

The p-value gives the probability for a background noise event to produce by chance L_{max} equal to or larger than the L_{max} of the candidate event (L_{ev}). Therefore, smaller p-values indicate the candidate is less likely to be a background noise event. A detection is declared if the p-value of a candidate is less than a certain threshold value p_0, which is chosen according to the required statistical significance for detections.

3. Monte Carlo simulation

In order to demonstrate our analysis pipeline, we performed Monte Carlo simulations. We first generated a LIGO event list using 17.6 hours of LIGO-like data which has similar statistical properties (such as the standard deviation, the glitch rate, etc.) to the real LIGO data during the fifth scientific run (S5) [29]. Using the statistics of LIGO events obtained from this list (i.e. the event rate and the distributions of τ and $\delta\tau$ used below), we generated a large number of background LIGO events by Monte Carlo. For each event, a trigger time was assigned randomly with the event rate of 13.4 events per day. The arrival time difference τ between the two LIGO sites was
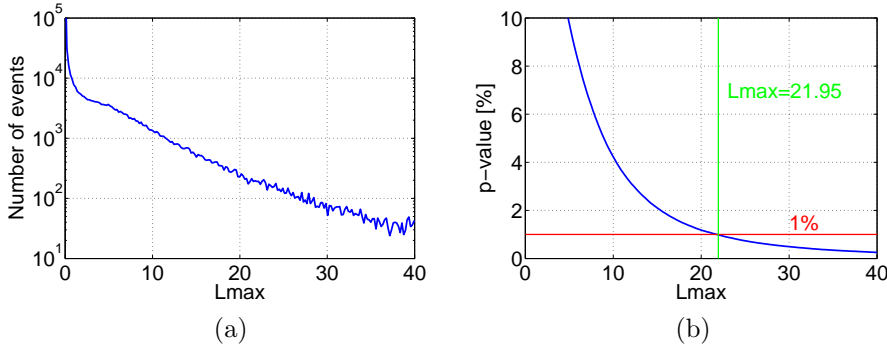
(a)

(b)

Figure 3. (a) The histogram of $L_{\max}$ for background events. (b) The plot of p-value as a function of $L_{\max}$. The false event detection probability (p-value) of 1 % corresponds to $L_{\max} = 21.95$. Detection is declared when the $L_{\max}$ of a candidate event is above this threshold.

distributed uniformly between -10 msec and 10 msec. The uncertainty $\delta\tau$ of the time difference was generated following the gamma distribution below:

$$P_{\delta\tau}(\delta\tau) = \frac{1}{b^a \Gamma(a)} (\delta\tau)^{a-1} e^{-\delta\tau/b}, \tag{7}$$

$$a = 1.93, \quad b = 4.41 \times 10^{-4}.$$

This distribution was chosen by a fit to the histogram of $\delta\tau$ obtained from the LIGO-like data.

Simulated IceCube events are distributed uniformly over the northern hemisphere of the sky with event rate of 2 events per day. This event rate corresponds to the one obtained during the operation of IceCube in nine-string configuration from June to November of 2006 [17]. No IceCube events from the southern sky are generated because they are rejected by the IceCube event reconstruction algorithm to avoid contamination by cosmic ray muons. The uncertainty σ_ν of event direction is set to be a constant value of 2°, which is the median angular reconstruction error of IceCube in the nine-string configuration.

The simulated LIGO and IceCube events are fed into our analysis pipeline. Figure 3 (a) shows the histogram of the background $L_{\max}$. By integrating the histogram, we get the relation between p-value and $L_{\max}$ (Figure 3 (b)). From this plot, we can determine the detection threshold for $L_{\max}$. For example, in order to require the chance of false event detection (p-value) to be less than 1 %, the corresponding $L_{\max}$ is 21.95. Detection is declared when the $L_{\max}$ of a candidate event is above this threshold.

4. Discussion

For each LIGO event, the expected number of IceCube event found within a time window ($\pm T_{\mathrm{W}}$) is $2T_{\mathrm{W}} \cdot R_\nu$, where R_ν is the event rate of IceCube. Therefore, using the event rate R_{GW} of LIGO, the survival rate for the LIGO-IceCube time coincidence can be calculated by $2T_{\mathrm{W}} \cdot R_{\mathrm{GW}} \cdot R_\nu$. Since the p-value threshold p_0 is the survival

rate of the spatial coincidence for background events, the FAR of this analysis method can be expressed by the following formula,

$$\text{FAR} = 2T_\text{W} \cdot R_\text{GW} \cdot R_\nu \cdot p. \tag{8}$$

More specifically in the case of the Monte Carlo simulation explained in the previous section, the FAR is given by the following formula,

$$\text{FAR} = \frac{1}{435} \left(\frac{p}{1\,\%} \right) \left(\frac{T_\text{W}}{1\,\text{sec}} \right) \text{ [events/year].} \tag{9}$$

The obtained typical FAR (1 event per 435 years) for 1 sec time window is smaller than the widely accepted SNEWS (SuperNova Early Warning System) standard (1 event per 100 years) [30]. This small FAR would allow us to relax the trigger generation thresholds of the individual detectors to dig deeper into the background noise while keeping compliance to the SNEWS standard.

In the case of long GRBs, high energy neutrinos from relativistic shocks are expected to be emitted about a few hours (for the internal shocks [24, 31, 32]) to a few days (for the external shocks [33]) after gravitational wave emission caused by core bounce. In order to look for this type of events, we have to use a large time window of order of days. In this case, we may not be able reject background events by time coincidence because the current event rate of more than one event per day for both detectors will allow most LIGO events to find at least one companion IceCube event (and vice versa) within a day. This means most events in trigger lists will survive the time coincidence. However, even in this case, time coincidence is necessary to form pairs of LIGO-IceCube events to be processed for spatial coincidence in the next step. On the other hand, the time coincidence is effective to search for GW and neutrino bursts with small time delay.

Our method can also be applied to coincidence analyses with other neutrino detectors such as Super-Kamiokande [34], Lake Baikal [35], Baksan [36] etc, without a significant modification. Moreover, our method can be used with any astronomical detectors which provide timing and source location information of burst events. Coincidence search with a large number of detectors will increase the confidence of detections.

We shall extend our method to include the VIRGO gravitational wave detector. The use of three geographically separated interferometers will enable us to constrain possible source locations of a gravitational wave event to two points on the sky [37]. Additionally, time coincidence discrimination between VIRGO and LIGO interferometers will further reduce the background event rate of the gravitational wave detectors network. This will provide us with stricter spatial coincidence and a lower FAR and/or higher sensitivity.

References

[1] S. A. Hughes, S. Márka, P. L. Bender, and C. J. Hogan. New physics and astronomy with the new gravitational-wave observatories. In *Proceedings of the 2001 Snowmass Meeting*, page 402, 2001.

[2] D. Sigg and the LIGO Science Collaboration. *Classical and Quantum Gravity*, **23**:S51–S56, 2006.

[3] R. Takahashi and TAMA Collaboration. *Classical and Quantum Gravity*, **21**:S403–S408, 2004.

[4] H. Lück *et al. Classical and Quantum Gravity*, **23**:S71–S78, 2006.

[5] F. Acernese *et al. Classical and Quantum Gravity*, **23**:S63–S69, 2006.

[6] B. Abbott *et al. Classical and Quantum Gravity*, **23**:29, 2006.

[7] B. Abbott *et al. Phys. Rev. D*, **69**(10):102001, 2004.

[8] B. Abbott *et al. Phys. Rev. D*, **72**(12):122004, 2005.

[9] S. Márka and L. Matone. Searching for Cataclysmic Cosmic Events with a Coincident Gamma-ray Burst and Gravitational Wave Signature. In S. S. Holt, N. Gehrels, and J. A. Nousek, editors, *Gamma-Ray Bursts in the Swift Era*, volume 836 of *American Institute of Physics Conference Series*, pages 605–611, 2006.

[10] The LIGO Scientific Collaboration. *Phys. Rev. D*, **76**:062003, 2007.

[11] S. Marka and S. D. Mohanty. *Nucl. Phys. Proc. Suppl.*, **138**:446–448, 2005.

[12] S. D. Mohanty *et al. Class. Quant. Grav.*, **21**:S765–S774, 2004.

[13] N. Arnaud, M. Barsuglia, M.-A. Bizouard, V. Brisson, F. Cavalier, M. Davier, P. Hello, S. Kreckelbergh, and E. K. Porter. *Astroparticle Physics*, **21**:201–221, 2004.

[14] A. Abramovici, W. E. Althouse, R. W. P. Drever, Y. Gursel, S. Kawamura, F. J. Raab, D. Shoemaker, L. Sievers, R. E. Spero, and K. S. Thorne. *Science*, **256**:325–333, 1992.

[15] R. E. Frey. LIGO: Status and Recent Results. In *American Institute of Physics Conference Series*, volume 928 of *American Institute of Physics Conference Series*, pages 11–22, 2007.

[16] J. Ahrens *et al. Astroparticle Physics*, **20**:507–532, 2004.

[17] C. Finley, J. Dumm, and T. Montaruli. Nine-string icecube point source analysis. In *Proceedings of 30th International Cosmic Ray Conference (ICRC)*, in press, 2007.

[18] N. Gehrels *et al. Astrophys. J.*, **611**:1005–1020, 2004.

[19] S. Campana *et al. Nature*, **442**:1008–1010, 2006.

[20] D. Lazzati. Gamma-Ray Burst Progenitors Confront Observations. In M. Novello, S. Perez Bergliaffa, and R. Ruffini, editors, *The Tenth Marcel Grossmann Meeting. On recent developments in theoretical and experimental general relativity, gravitation and relativistic field theories*, page 860, 2005.

[21] S. E. Woosley and A. I. MacFadyen. *Astron. Astrophys. Sup.*, **138**:499–502, 1999.

[22] K. Kotake, K. Sato, and K. Takahashi. *Reports of Progress in Physics*, **69**:971–1143, 2006.

[23] T. Piran. *Rev. Mod. Phys.*, **76**:1143–1210, 2005.

[24] E. Waxman and J. Bahcall. *Phys. Rev. Lett.*, **78**:2292–2295, 1997.

[25] M. Vietri. *Phys. Rev. Lett.*, **80**:3690–3693, 1998.

[26] W. H. Lee and E. Ramirez-Ruiz. *New J. Phys.*, **9**:17, 2007.

[27] F. Beauville *et al. Classical and Quantum Gravity*, **22**(18):S1293, 2005.

[28] S. Chatterji, L. Blackburn, G. Martin, and E. Katsavounidis. *Classical and Quantum Gravity*, **21**(20):S1809, 2004.

[29] S. J. Waldman and the LIGO Science Collaboration. *Classical and Quantum Gravity*, **23**:3, 2006.

[30] Pietro Antonioli *et al. New Journal of Physics*, **6**:114, 2004.

[31] Nayantara Gupta and Bing Zhang. *Astroparticle Physics*, **27**(5):386, 2007.

[32] K. Murase and S. Nagataki. *Physical Review Letters*, **97**(5):051101, 2006.

[33] Eli Waxman and John N. Bahcall. *Astrophys. J.*, **541**:707–711, 2000.

[34] Y. Fukuda *et al. Nuclear Instruments and Methods in Physics Research Section A*, **501**:418–462, 2003.

[35] R. Wischnewski. *ArXiv Astrophysics e-prints*, 2006.

[36] E. N. Alekseev *et al. Physics of Particles and Nuclei*, **29**:254–256, 1998.

[37] J. L. Boulanger, J. P. Duruisseau, G. Ledenmat, and P. Tourrenc. *Astron. Astrophys.*, **217**:381–386, 1989.